Disruption of the primocolonizing microbiota alters epithelial homeostasis and imprints stem cells in the colon of neonatal piglets

Martin Beaumont, Corinne Lencina, Katia Fève, Céline Barilly, Laurence Le-Normand, Sylvie Combes, Guillaume Devailly, Gaëlle Boudry

WILEY

Frontiers in Flow Cytometry™

24 hour Virtual Event

September 13th, 2023

Frontiers in Flow Cytometry™ is for researchers across the globe looking for an opportunity to share and learn about current developments in flow cytometry. This 24 hour virtual event will feature keynote presentations by industry colleagues, webinars, demos, live networking opportunities and more.

Key topics include:

- Spectral and conventional flow cytometry
- Immunophenotyping and Standardization
- Panel design and optimization
- Cancer Biology and Auto-immune Diseases
- Infectious diseases
- Advances in flow cytometry technology

Register Now

This event is sponsored by **Thermo Fisher** SCIENTIFIC

RESEARCH ARTICLE

The FASEB Journal

Disruption of the primocolonizing microbiota alters epithelial homeostasis and imprints stem cells in the colon of neonatal piglets

Martin Beaumont[1] | **Corinne Lencina**[1] | **Katia Fève**[1] | **Céline Barilly**[1] | **Laurence Le-Normand**[2] | **Sylvie Combes**[1] | **Guillaume Devailly**[1] | **Gaëlle Boudry**[2]

[1]GenPhySE, Université de Toulouse, INRAE, ENVT, Castanet-Tolosan, France

[2]Institut NuMeCan, INRAE, INSERM, Univ Rennes, Saint-Gilles, France

Correspondence
Martin Beaumont, GenPhySE, Université de Toulouse, INRAE, ENVT, Castanet-Tolosan, France.
Email: martin.beaumont@inrae.fr

Funding information
INRAE (HOLOFLUX)

Abstract

The gut microbiota plays a key role in the postnatal development of the intestinal epithelium. However, the bacterial members of the primocolonizing microbiota driving these effects are not fully identified and the mechanisms underlying their long-term influence on epithelial homeostasis remain poorly described. Here, we used a model of newborn piglets treated during the first week of life with the antibiotic colistin in order to deplete specific gram-negative bacteria that are transiently dominant in the neonatal gut microbiota. Colistin depleted Proteobacteria and Fusobacteriota from the neonatal colon microbiota, reduced the bacterial predicted capacity to synthetize lipopolysaccharide (LPS), and increased the concentration of succinate in the colon. The colistin-induced disruption of the primocolonizing microbiota was associated with altered gene expression in the colon epithelium including a reduction of toll-like receptor 4 (TLR4) and lysozyme (LYZ). Our data obtained in porcine colonic organoid cell monolayers suggested that these effects were not driven by the variation of succinate or LPS levels nor by a direct effect of colistin on epithelial cells. The disruption of the primocolonizing microbiota imprinted colon epithelial stem cells since the expression of TLR4 and LYZ remained lower in organoids derived from colistin-treated piglet colonic crypts after several passages when compared to control piglets. Finally, the stable imprinting of LYZ in colon organoids was independent of the H3K4me3 level in its transcription start site. Altogether, our results show that disruption of the primocolonizing gut microbiota alters epithelial innate immunity in the colon and imprints stem cells, which could have long-term consequences for gut health.

KEYWORDS

colistin, epigenetics, gut microbiota, lipopolysaccharide, lysozyme, metabolites, monolayers, organoids, succinate, toll-like receptor 4

Abbreviations: AQP8, aquaporin 8; CFTR, cystic fibrosis transmembrane conductance regulator; ChIP, chromatin immunoprecipitation; FABP1, fatty acid binding protein 1; H3K4me3, trimethylation of histone H3 lysine 4; LBP, LPS-binding protein; LPS, lipopolysaccharide; LYZ, lysozyme; NMR, nuclear magnetic resonnance; NOX1, NADPH oxidase 1; OLFM4, Olfactomedin 4; PCNA, proliferation cell nuclear antigen; PYY, peptide YY; TEER, transepithelial electrical resistance; TLR4, toll-like receptor 4; TSS, transcription start site.

1 | INTRODUCTION

The function of the intestinal epithelium is digestion and absorption of nutrients while forming a barrier against pathogens and toxic compounds potentially present in the gut lumen.[1] This dual function is performed by diverse epithelial lineages, including absorptive cells and secretory cells involved in the production of mucus, antimicrobial peptides, or enterohormones.[2] All these differentiated epithelial cells derive from long-lived stem cells located at the base of crypts.[3] The rapid proliferation of epithelial progenitors allows the complete renewal of the intestinal epithelium within a few days without compromising its barrier function. Disruption of these processes can lead to inflammatory and infectious diseases, especially when the intestinal epithelium is still developing.[4] It is, therefore, essential to understand the mechanisms involved in the regulation of epithelial homeostasis in early life.

The gut microbiota that rapidly develops after birth strongly influences the functionality of the intestinal epithelium.[4] Indeed, neonatal antibiotic administration disturbs epithelial architecture, proliferation, and differentiation of goblet and Paneth cells, and alters barrier function.[5–8] Moreover, microbial colonization at birth rapidly alters transcription and epigenomic landscape in intestinal epithelial cells.[9,10] The production of bacterial metabolites is thought to play a central role in the microbial control of epithelial development in early life.[11–13] For instance, the neonatal microbiota regulates intestinal epithelial proliferation through the production of lactate that activates the Wnt/β-catenin pathway in intestinal epithelial stem cells.[14] Short-chain fatty acids produced by the early life microbiota from milk oligosaccharides are also considered as drivers of epithelial maturation.[4,13] Importantly, gut microbiota-derived metabolites can induce epigenetic modifications in intestinal epithelial cells and thereby influence epithelial functions in the long term.[15,16] Although the involvement of the microbiota in the development of the intestinal epithelium in early life is well established, the specific bacterial groups involved in these processes remain to be identified.

The initial colonization of the neonatal gut by facultative anaerobe, mainly Proteobacteria, is a typical step of the microbiota development linked to the relatively high abundance of oxygen in the intestine at birth.[17] For instance, *Enterobacteriaceae* is a dominant family of the gut microbiota in human neonates and its abundance rapidly declines with postnatal development.[17–21] A study in mono-colonized rats revealed that, among several primocolonizing bacteria tested, *Escherichia coli*, member of the *Enterobacteriaceae* family, plays a predominant role in triggering epithelial maturation induced by bacterial colonization.[22] Thus, we hypothesized that such bacterial groups transiently dominating the gut microbiota during the neonatal period could play a key role in the crosstalk with the developing intestinal epithelium.

Pig is an excellent model to study the neonatal physiology of the intestine due to anatomical and microbiota similarities with humans.[23,24] Indeed, fully formed intestinal epithelial crypts are already present at birth in pigs and humans while they are structurally and functionally mature only 2 weeks after birth in mice.[25] In this study, we investigated the consequences of the depletion of a dominant fraction of the primocolonizing microbiota on colon epithelial homeostasis by using a model of neonatal piglets treated with colistin, an antibiotic targeting specific gram-negative bacteria such as *Enterobacteriaceae*. We show that the colistin-induced depletion of Proteobacteria and Fusobacteriaceae during the first week of life alters epithelial innate immune responses and imprints colon epithelial stem cells which might have potential long-term consequences for gut health.

2 | MATERIALS AND METHODS

2.1 | Animals and sample collection

Animal experiment was conducted in accordance with the current ethical standards of the European Community (Directive 2010/63/EU) and animal facility agreement No. D3527532. The Rennes Ethics Committee in Animal Experiment and the French Ministry of Higher Education and Research approved and authorized the entire procedure (project number APAFIS # 26559-2020061708436243 v4).

Six large white x landrace sows from INRAE facility (UE3P, Saint-Gilles, France) were assigned to either the colistin ($n=3$ litters) or vehicle ($n=3$ litters) group. Six suckling piglets per litter (three males and three females, birth weight 1.45 ± 0.05 kg) were weighed and received daily by oral gavage either water (1 mL/piglet, vehicle group) or colistin sulfate (Biove Vetocoli, 200 000 IU/kg dissolved in water, colistin group) from birth to 7 days of age. This dosage was chosen based on veterinary practice for the treatment of gastrointestinal infection in piglets.[26] At 7 days of age, piglets were euthanized by electronarcosis immediately followed by bleeding.

After laparotomy, sections of 5 cm of proximal colon were isolated, opened longitudinally, and thoroughly rinsed with ice-cold PBS with 5 mM dithiothreitol (DTT, Sigma-Aldrich D-5545) and 1% penicillin-streptomycin-amphotericin (PSA, Sigma-Aldrich A-5955). Each section was then pinned on a sylgard-coated petri dish, apical side up and the mucus was removed by gently scraping with angled forceps under a binocular magnifying glass.

Tissues were then incubated for 30 min on a shaking plate (80 rpm) in a dissociation solution composed of 10 mL of PBS supplemented with 3 mM DTT, 1% PSA, 9 mM EDTA (Sigma-Aldrich, E-7889), and 10 μM of Y27632 (Preprotech #1293823). The dissociation solution was then removed and replaced with 10 mL of PBS supplemented with 1% PSA and 10 μM Y27632. Each sample was scraped using angled forceps under a binocular magnifying glass in order to release the crypts. The isolated crypts were filtered at 200 μm, centrifuged at 100 g, 4°C for 5 min, and either resuspended in DMEM/F12 (Gibco #12634) supplemented with 10% fetal bovine serum (FBS) and 10% dimethylsulfoxide (Sigma D-2650) and immediately frozen at −80°C in a CoolCell for 24 h before long-term storage at −150°C for later organoid culture or stored at −80°C for later RNA extraction.

2.2 | 16S rRNA gene amplicon sequencing and sequence analysis

DNA was extracted from 50 mg of piglet colon content using the Quick-DNA Fecal/Soil Microbe 96 Kit (ZymoResearch) according to the manufacturer's instructions. PCR amplicons of the 16S rRNA gene V3-V4 region were sequenced by MiSeq technology (Illumina) at the Genomic and transcriptomic platform (GeT-PlaGe, INRAE, Toulouse), as described before.[27] Sequencing reads were deposited in the National Center for Biotechnology Information Sequence Read Archive (accession number: PRJNA933391). Amplicon sequences were analyzed by the FROGS pipeline version 3.2.3,[28] following the guidelines. Merged sequences were selected based on their size (350–500 nucleotides), dereplicated, and counted. Sequences were then clustered into OTUs by using Swarm (clustering aggregation distance: 1). After PCR chimera removal, the OTUs present in less than three samples or whose proportion represented less than 0.005% of all sequences were filtered out. The taxonomic affiliation of OTUs was performed with the 16S SILVA database (138.1, pintail 100). A phyloseq object with OTU count table and sample metadata was created. The mean number of reads per sample was 17 859 (min: 14454-max: 26522). For α and β-diversity analyses, the count table was rarefied to 14 454 sequences per sample with the R software (4.2.0) and the phyloseq package (1.40.0). Microbiota richness (number of observed OTUs) and Shannon and Inverse Simpson α-diversity index were calculated. β-diversity was analyzed with the distance of Bray-Curtis and visualized by non-metric multidimensional scaling (nMDS). The unrarefied count table was used to calculate the relative abundances of bacterial taxa at the phylum, family, and genus levels. The functional potential of the gut microbiota was predicted with PICRUSt2[29] as implemented in FROGS (functional analysis tools) and according to the guidelines.[30] OTUs were placed in the PICRUSt2 reference tree with epa-ng with a minimum alignment length of 80%. Hidden state prediction was performed with the maximum parsimony method with MetaCyc EC-Numbers. OTUs with a nearest sequenced taxon index (NSTI) > 0.2 were excluded from analysis to improve accuracy of prediction. Thus, 402 OTUs representing 88% of the total number of sequences were used for functional predictions. For each sample, the abundances of MetaCyc pathways were calculated and normalized by the total abundance of all pathways to account for differences in sequencing depth.

2.3 | Nuclear magnetic resonance-based metabolomics

Colon content samples (50 mg) were homogenized in 500-μL phosphate buffer (pH 7, prepared in D_2O, containing 1 mM TSP used as a chemical shift reference) with a FastPrep instrument and using tubes containing lysing D matrix (MP Biomedicals). After centrifugation (12 000 g, 10 min, 4°C), the supernatant containing metabolites was recovered and the extraction step was repeated on the pellet. The two fractions of supernatant were pooled and then centrifuged twice (18 000 g, 10 min, 4°C). The obtained supernatants (600 μL) were transferred to 5-mm nuclear magnetic resonance (NMR) tubes. All NMR spectra were obtained with an Avance III HD NMR spectrometer operating at 600.13 MHz for ^1H resonance frequency using a 5-mm inverse detection CryoProbe (Bruker Biospin, Rheinstetten, Germany) in the MetaboHUB-MetaToul-AXIOM metabolomics platform (Toulouse, France). ^1H NMR spectra were acquired at 300 K using the Carr-Purcell-Meiboom-Gill spin-echo pulse sequence with pre-saturation. Pre-processing of the spectra (group delay correction, solvent suppression, apodization with a line broadening of 0.3 Hz, Fourier transform, zero-order phase correction, shift referencing on TSP, baseline correction, setting of negative values to zero) was performed in the Workflow4Metabolomics Galaxy tool following guidelines.[31] After water region (4.5–5.1 ppm) exclusion, spectra (0.5–9 ppm) were bucketed (0.01 ppm bucket width) and normalized by total area. Representative samples were characterized by 2D NMR experiments (^1H-^1H COSY). For metabolite identification, 1D and 2D NMR spectra of pure compounds prepared in the same buffer and acquired with the same spectrometer were overlayed with colon sample spectra. A representative annotated spectrum is presented in

Figure S1. For each identified metabolite, a bucket non-overlapping with other metabolites was selected for the quantification (Table S1). The relative concentrations of metabolites were calculated by dividing the bucket area measured in each sample by the mean of bucket area measured in control piglets.

2.4 | Histology

Transverse sections of colon were fixed in 4% buffered paraformaldehyde at room temperature for 24 h, rinsed in three 70% ethanol 1-h baths, embedded in paraffin, and sections were stained with Alcian blue and Periodic Acid Schiff at the histology platform ANEXPLO (Genotoul, Toulouse, France). Slides were digitalized and crypt depth and epithelial cell height were measured with the CaseViewer 2.3 software (3DHISTECH).

2.5 | Culture of organoids from cryopreserved colon epithelial crypts

Crypts were rapidly thawed and washed with warm PBS. Crypts were then seeded in Matrigel (Matrigel Growth Factor Reduced Basement Membrane Corning #CLS356239) droplets (300 crypts/50 μL Matrigel/well) in pre-warmed plates. The plates were then placed at 37°C for 20 min to allow Matrigel polymerization before the addition of 500 μL of IntestiCult Organoid Growth Medium (Human) (Stemcell Technologies, #06010) supplemented with 10 μM Y27632 and 1% PSA. Organoids were cultured in an incubator at 37°C, 5% CO_2, and 90% humidity. The medium was renewed after 24 h by removing Y27632 and then every 48 h. Organoids were passaged at a 1:4 ratio between the 7th and 15th day of primary culture when they presented a sufficient size (>150 μm) and a budding appearance. For passaging, the medium culture was replaced by 750 μL of Gentle Cell Dissociation Reagent (GCDR, StemCell Technologies #100-0485). Matrigel domes were mechanically dissociated by scratching and pipetting the GCDR solution. The operation was repeated once in order to recover all the organoids from the well. The tubes containing the GCDR solution and organoids were incubated on a shaking plate for 10 min at 40 rpm at room temperature and then centrifuged at 290 g, 4°C for 5 min. The organoids were then suspended in DMEM-F12 supplemented with 1% PSA and 1% FBS, filtered at 70 μm, and resuspended into a new Matrigel dome as described above. Organoids were passaged a second time after 7–10 days of culture. They were then harvested as described for passaging, rinsed in PBS once, and immediately frozen at −80°C

with lysis buffer until RNA purification, as described below.

2.6 | Colon organoid cell monolayers derived from newborn piglets

The colon of five piglets was collected immediately after vaginal birth (<30 min after birth, with no access to colostrum during these 30 min) and epithelial crypts were isolated and cryopreserved as described above. Cell monolayers derived from the colon organoids of newborn piglets were cultured as described previously.[32] One day after cell seeding, the basolateral medium was replaced by IntestiCult Organoid Growth Medium Human supplemented with 1% Penicillin/Streptomycin and treatments were added at the apical side. All treatments were prepared in IntestiCult Organoid Growth Medium (Human) supplemented with 1% Penicillin/Streptomycin. Succinate (Sigma-Aldrich, 14160) was used at 0.1, 1, and 10 mM according to the concentration range used in other publications.[33–35] LPS from *Escherichia coli* O111:B4 (Sigma-Aldrich, L2630) was used at 0.1, 1, and 10 μg/mL based on previous studies in intestinal organoids.[36–38] Colistin sulfate (Biove, Vetocoli) was used at 1, 10, and 100 μg/mL based on quantification of colistin in the gastrointestinal tract of piglets treated with this antibiotic.[26,39,40] The treatments were refreshed after 24 h. Transepithelial electrical resistance (TEER) was measured with an Epithelial Volt Ohm Meter (EVOM3, World Precision Instruments) according to the manufacturer's instructions. Cells were lyzed in TRI Reagent (ZymoResearch) and stored at −80°C until RNA extraction.

2.7 | Gene expression in colon epithelial crypts and in colon organoids

Total RNA was extracted from isolated epithelial crypts with the kit Direct-zol RNA MiniPrep Plus (ZymoResearch) according to the manufacturer's instructions. RNA from 3D organoids was extracted using the RNeasy Micro Kit (Qiagen) following manufacturer's instructions. Retrotranscription of total RNA (500 ng for organoids and 1 μg for crypts) to cDNA was performed with the kit GoScript™ Reverse Transcription Mix, Random Primers (Promega). mRNA levels of target genes were quantified by quantitative PCR by using specific primers (Table S2). Gene expressions were quantified by Power SYBR Green PCR Master Mix (Fischer Scientific) with QuantStudio 6 Flex Real-Time PCR System (ThermoFisher) or by using Dynamic Array Integrated

Fluidic Circuit with a BioMark System (Fluidigm) following the manufacturer's instructions. Specificity of PCR products was verified by melt curve examination. For each gene, the cycle threshold (CT) was determined and used to calculate the relative mRNA level by using the $2^{-(CT\ gene\ of\ interest\ -\ CT\ housekeeping\ gene)}$ method. Housekeeping genes were selected based on the stability of their expression between groups (RPL32 for crypts, HMBS for 3D organoids, and GAPDH for organoid cell monolayers). mRNA levels were then normalized to the expression value in the control group.

2.8 | Chromatin immunoprecipitation (ChIP)-qPCR

Colon organoid lines derived from three control and three colistin-treated piglets were selected based on their high and low expression of LYZ in crypts (in vivo) and at passage 2. The selected organoids cryopreserved after two passages were thawed and cultured for two additional passages (P3 and P4) as described above. Organoids at P3 and P4 were lyzed in TRI Reagent (ZymoResearch) for quantification of LYZ mRNA expression by qPCR, as described above. Organoids at P4 were dissociated into single cells 7 days after seeding by pipetting after incubation in warm EDTA-trypsin 0.25% w/v for 15 min at 37°C. ChIP targeting H3K4me3 was performed with 500 000 cells from each organoid line with the True MicroChIP-seq Kit (Diagenode, Cat#C01010132) following the manufacturer's instructions. Protein-DNA were cross-linked for 8 min with 1% paraformaldehyde before quenching with glycine, cell lysis, and fragmentation of the cross-linked chromatin using a Bioruptor Pico (Diagenode) with six cycles (30 s ON/OFF). An input of each sample was saved before immunoprecipitation. H3K4me3-DNA complexes were immunoprecipitated with an antibody targeting H3K4me3 (0.5 μg per reaction, provided in the kit) and protein-A magnetic beads. Cross-links were reversed and DNA was purified using DiaPure columns and eluted in 35 μL DNA elution buffer. qPCR was performed on input (diluted 1:10) and immunoprecipitated DNA with primers targeting the transcription start site (TSS) LYZ (F: 5′-CCAGAGCTCCGAGACAACAG-3′, R: 5′-CGGCGGTT TCTTTTGTGTGT-3′) and an intronic region of LYZ (F: 5′-CCATACGGAGGCCAGAAGAC-3′, R: 5′-GGAGT TGAAGCGACACTCCT-3′), used as a negative control. qPCR was performed using a QuantStudio 6 Flex Real-Time PCR System (Thermo Fisher Scientific). The percentage of total chromatin input was calculated for each region (LYZ TSS or intron) with the following formula: $\%\ input = 10 \times 2^{(CT_{input}\ -\ CT_{H3K4me3})}$.

2.9 | Statistical analysis

The R software (4.2.0) was used for statistical analyses. In vivo data were analyzed by linear mixed models (lme4 and car packages) after the transformation of data to the power of 0.25. Models included the group as a fixed effect (control or colistin) and the litter as a random effect. *p*-Values were corrected for multiple testing using the Benjamini-Hochberg method for microbiota and metabolomics data. Statistical analyses were performed only for bacterial taxa in which relative abundance was over 0.5% within at least one group since this threshold was previously shown to ensure reproducible quantifications by 16S rRNA gene amplicon sequencing.[41] PERMANOVA with 999 permutations was used to study the effects of group and litter on the microbiota structure (vegan package). Principal component analysis (PCA) was performed with the mixOmics package. Data obtained in 3D organoids derived from control or colistin-treated piglets were analyzed by linear mixed models with the group as a fixed effect and the litter as a random effect. Data obtained in organoid cell monolayers were analyzed by linear mixed models with the group as a fixed effect and the piglet as a random effect.

3 | RESULTS

3.1 | Colistin disrupted the primocolonizing microbiota in the colon of neonatal piglets

In order to alter the primocolonizing gut microbiota, we treated piglets orally every day during the first week of life with colistin, an antibiotic poorly absorbed in the intestinal tract acting on gram-negative bacteria through its binding to the lipid A portion of LPS molecules[42] (Figure 1A). The colistin treatment had no effect on piglet growth (mean body weight ± s.e.m at day 7: 2.73 kg ± 0.17 and 2.84 kg ± 0.18 in the control and colistin groups, respectively). Colistin did not reduce the colon microbiota richness and diversity at postnatal day 7 (Figure 1B and Table S3). However, β-diversity analysis revealed that colistin altered the microbiota structure (PERMANOVA: $R^2 = 12.5\%$, $p < .001$) (Figure 1C) which was, noteworthy, more strongly influenced by the litter (PERMANOVA: $R^2 = 38.4\%$, $p < .001$) (Figure S2A), as expected in the early neonatal period.[43,44] Colistin had a major effect on the relative abundance of a limited number of gram-negative bacterial taxa in the colon. Colistin depleted Proteobacteria (−92%) mostly through a reduction of *Enterobacteriaceae* (*Escherichia-Shigella*) and *Pasteurellaceae* (*Actinobacillus*) (Figure 1D,E and Table S3). Colistin also strongly reduced the abundance of Fusobacteriota, represented only by
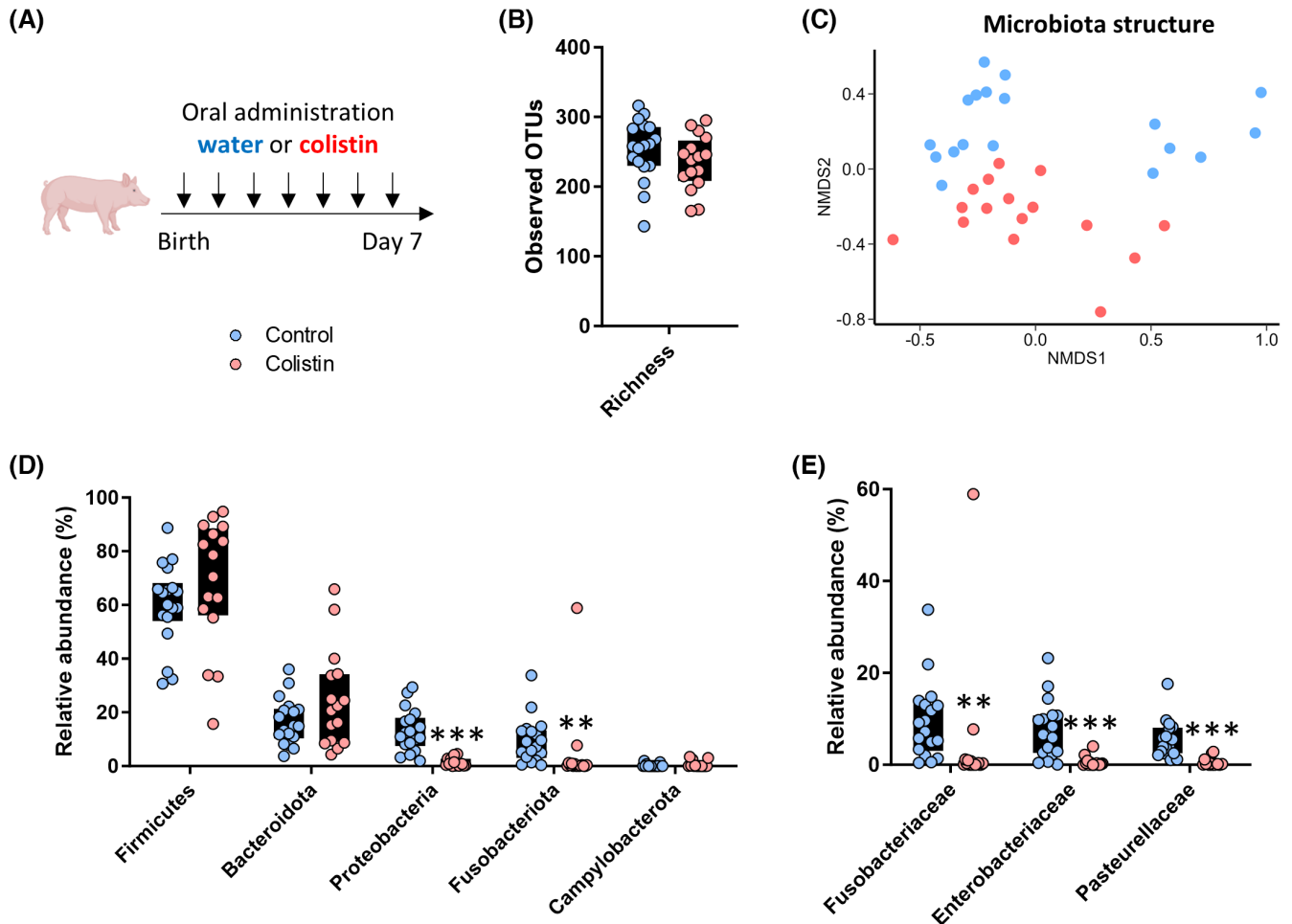
FIGURE 1 Proteobacteria and Fusobacteriota are depleted from the primocolonizing microbiota of neonatal piglets treated with colistin. Piglets were treated orally from birth to day 7 with colistin ($n = 16$) or water (control group, $n = 18$). The colon microbiota was analyzed by 16S rRNA gene amplicon sequencing. (A) Experimental design. (B) Microbiota Richness (number of observed OTUs). (C) Non-metric multidimensional scaling (nMDS) representation of the microbiota structure based on the Bray-Curtis distance (stress = 14.7). (D) Relative abundances of bacterial phyla. (E) Relative abundances of bacterial families. (B–E) Each dot represents an individual value. (B, D, E) Boxes extend from the 25th to the 75th percentiles. Significant differences are represented as ***$p < .001$, **$p < .01$ (colistin vs. control).

the genus *Fusobacterium*. In contrast, colistin increased the relative abundance of two bacterial families: *Muribaculaceae* and *Ruminococcaceae* (Table S3). Overall, our results show that colistin disrupted the primocolonizing microbiota in the colon of neonatal piglets, mainly by depleting Proteobacteria and Fusobacteriota.

3.2 | Disruption of the primocolonizing colon microbiota altered its metabolic functions

As a next step, we evaluated the functional consequences of the disruption of the primocolonizing microbiota induced by colistin. Functional inference based on 16S sequences revealed that the relative abundances of

predicted bacterial metabolic pathways were altered by colistin and by the litter, as illustrated by PCA (Figures 2A and S2B and Table S4). Consistently with the depletion of *Enterobacteriaceae*, colistin reduced the relative abundances of predicted metabolic pathways specific to this family, such as biosynthesis of LPS lipid A or enterobactin and enterobacterial common antigen (Figure 2B and Table S4). Colistin also reduced the relative abundance of predicted pathways involved in energy metabolism such as fatty acid oxidation, TCA cycle, or pyruvate fermentation (Table S4). Then, to further characterize the microbial metabolic shift induced by colistin, we performed metabolomics analysis in the colon contents (Table S5). We observed that colistin reduced the relative concentration of propionate while it increased the relative concentration of its precursor succinate
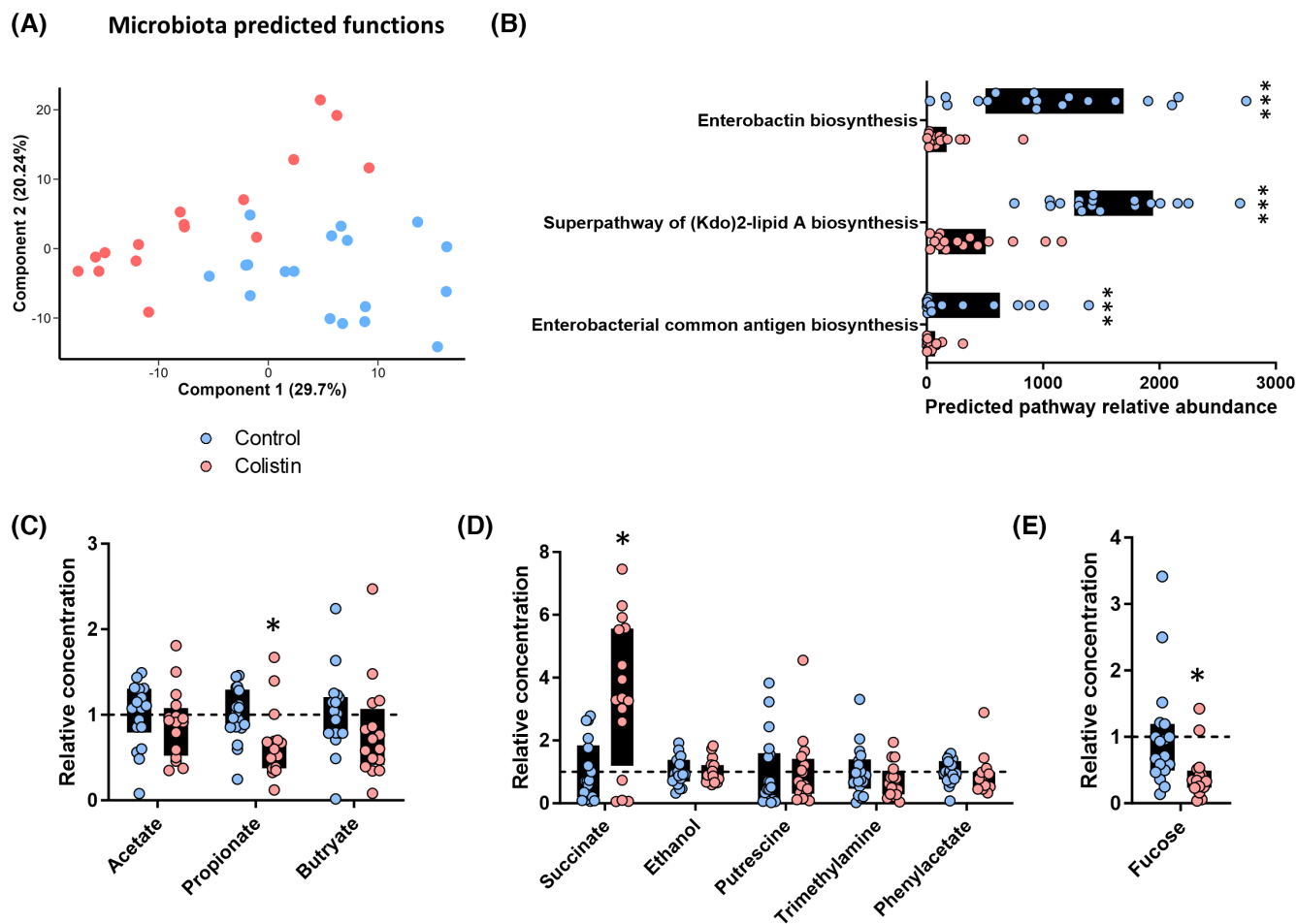
FIGURE 2 The metabolic activity of the primocolonizing microbiota is altered in neonatal piglets treated with colistin. Piglets were treated orally from birth to day 7 with colistin ($n = 16$) or water (control group, $n = 18$). (A, B) The functionality of the microbiota was predicted by inference from 16S rRNA gene amplicon sequences by using PICRUSt2. (A) Principal component analysis (PCA) representing the predicted functions of the colon microbiota (318 MetaCyc pathways). (B) Relative abundances of selected predicted MetaCyc pathways. (C–E) The colon metabolome was analyzed by nuclear magnetic resonance (NMR)-based metabolomics. Relative concentrations of short-chain fatty acids (C), other bacterial metabolites (D), and fucose (E). (A–E) Each dot represents an individual value. (B–E) Boxes extend from the 25th to the 75th percentiles. Significant differences are represented as ***$p < .001$, *$p < .05$ (colistin vs. control).

(3.5-fold increase) (Figure 2C,D). Interestingly, we also found that colistin reduced the relative concentration of fucose, which can be released by bacteria from mucins (Figure 2E). This result was associated with a reduction of the predicted capacity of the microbiota to degrade fucose in piglets treated with colistin (Table S4). Thus, our data indicate that the disruption of the primocolonizing microbiota by colistin led to an altered bacterial metabolism in the colon of neonatal piglets.

3.3 | Disruption of the primocolonizing microbiota alters epithelial functions in the colon

Since the microbiota and its metabolites play a key role in the postnatal development of the intestinal epithelium,

we next analyzed the effects of the disruption of the primocolonizing microbiota induced by colistin on colon epithelial cells. Histological analysis indicated that epithelial crypt depth and cell height were similar between piglets treated or not with colistin (Figure 3A). However, at the gene expression level, piglets treated with colistin expressed lower levels of the stem cell marker olfactomedin 4 (OLFM4) and of proliferation cell nuclear antigen (PCNA) (Figure 3B). Moreover, colistin treatment upregulated the differentiation marker aquaporin 8 (AQP8) while it reduced the expression of cystic fibrosis transmembrane conductance regulator (CFTR) and fatty acid binding protein 1 (FABP1), indicating an altered phenotype of absorptive epithelial cells (Figure 3C). The gene expression of the enterohormone peptide YY (PYY) was higher in piglets treated with colistin while markers of goblet cells remained unchanged (Figure 3C). These results suggest
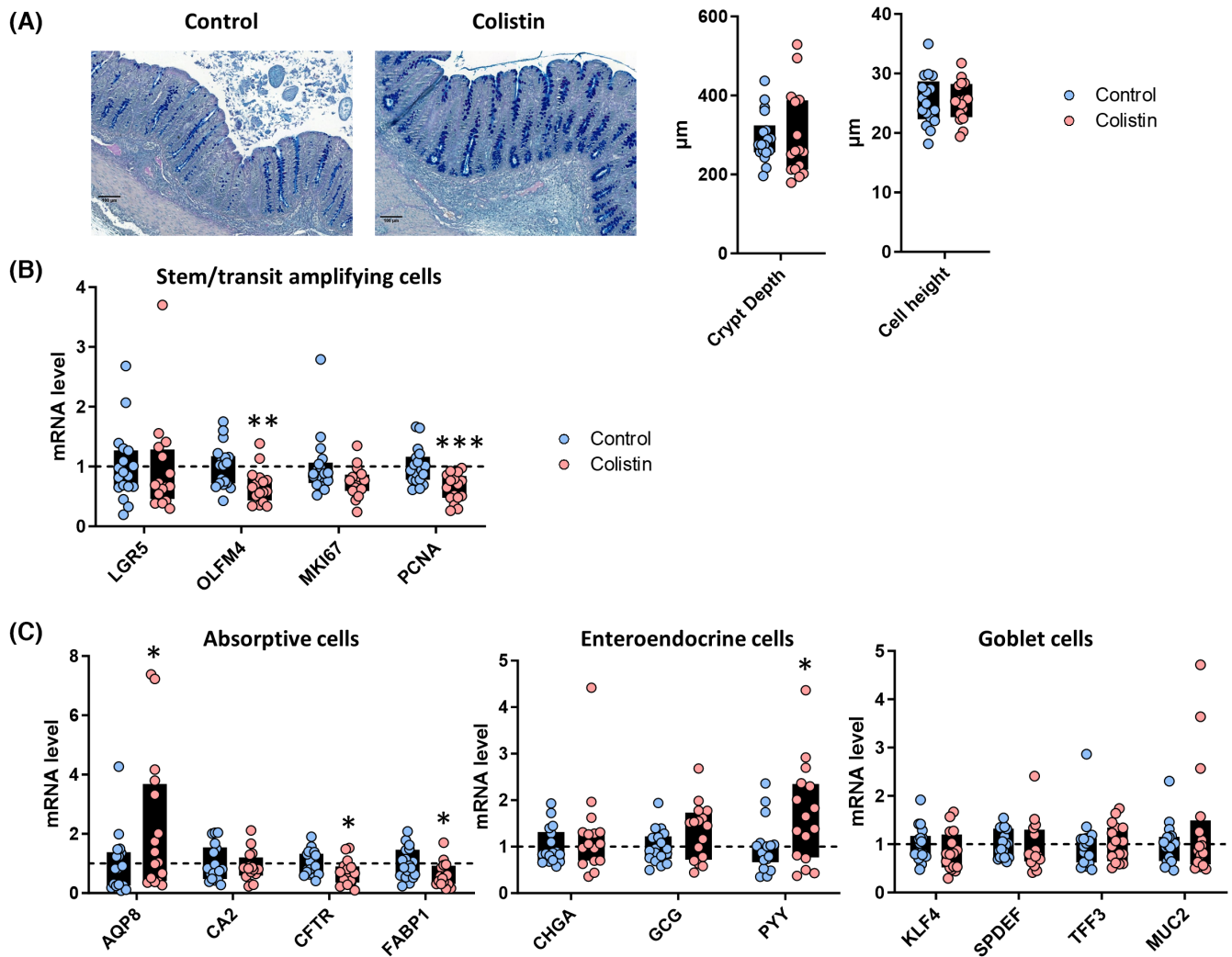
FIGURE 3 Epithelial gene expression is altered in the colon of neonatal piglets treated with colistin. Piglets were treated orally from birth to day 7 with colistin ($n = 16$) or water (control group, $n = 18$). (A) Colon sections were stained with Alcian blue and Periodic Acid Schiff. Representative observation of colon sections (scale bar: $100\,\mu m$). Crypt depth and epithelial cell height were measured. (B, C) Gene expression was analyzed by qPCR in colon epithelial cells. Relative expression of genes involved in epithelium renewal (B) or epithelial differentiation (C). (A–C) Each dot represents an individual value. Boxes extend from the 25th to the 75th percentiles. Significant differences are represented as *** $p < .001$, ** $p < .01$, * $p < .05$ (colistin vs. control).

that colistin altered the proliferation/differentiation balance in the colon epithelium of neonatal piglets.

Then, we focused on the epithelial barrier function that plays a central role in the host-microbiota crosstalk. Piglets treated with colistin expressed lower levels of genes coding for the LPS sensors toll-like receptor 4 (TLR4) and LPS binding protein (LBP) in the colon epithelium (Figure 4A), while the expression of other components of TLR signaling remained stable at the mRNA level. The expression of the antimicrobial peptide lysozyme (LYZ) was reduced in the colon epithelium of piglets treated with colistin (Figure 4B), while the expression of other antimicrobial peptides and cytokines remained unchanged (Figure 4B,C). Among enzymes involved in redox defenses, we observed a reduced expression of the pro-oxidant enzyme NADPH oxidase

1 (NOX1) in the epithelium of piglets treated with colistin (Figure 4D). The expression of genes coding for tight junction proteins was not changed by colistin treatment (Figure 4E). Altogether, our results show that the modification of the primocolonizing microbiota induced by colistin was associated with a reduced gene expression of major regulators of innate defenses in the colon epithelium.

3.4 | Evaluation of the direct effects of succinate, LPS, and colistin on colon epithelial cells of newborn piglets

The observed modifications of epithelial functions upon colistin treatment were most likely due to the
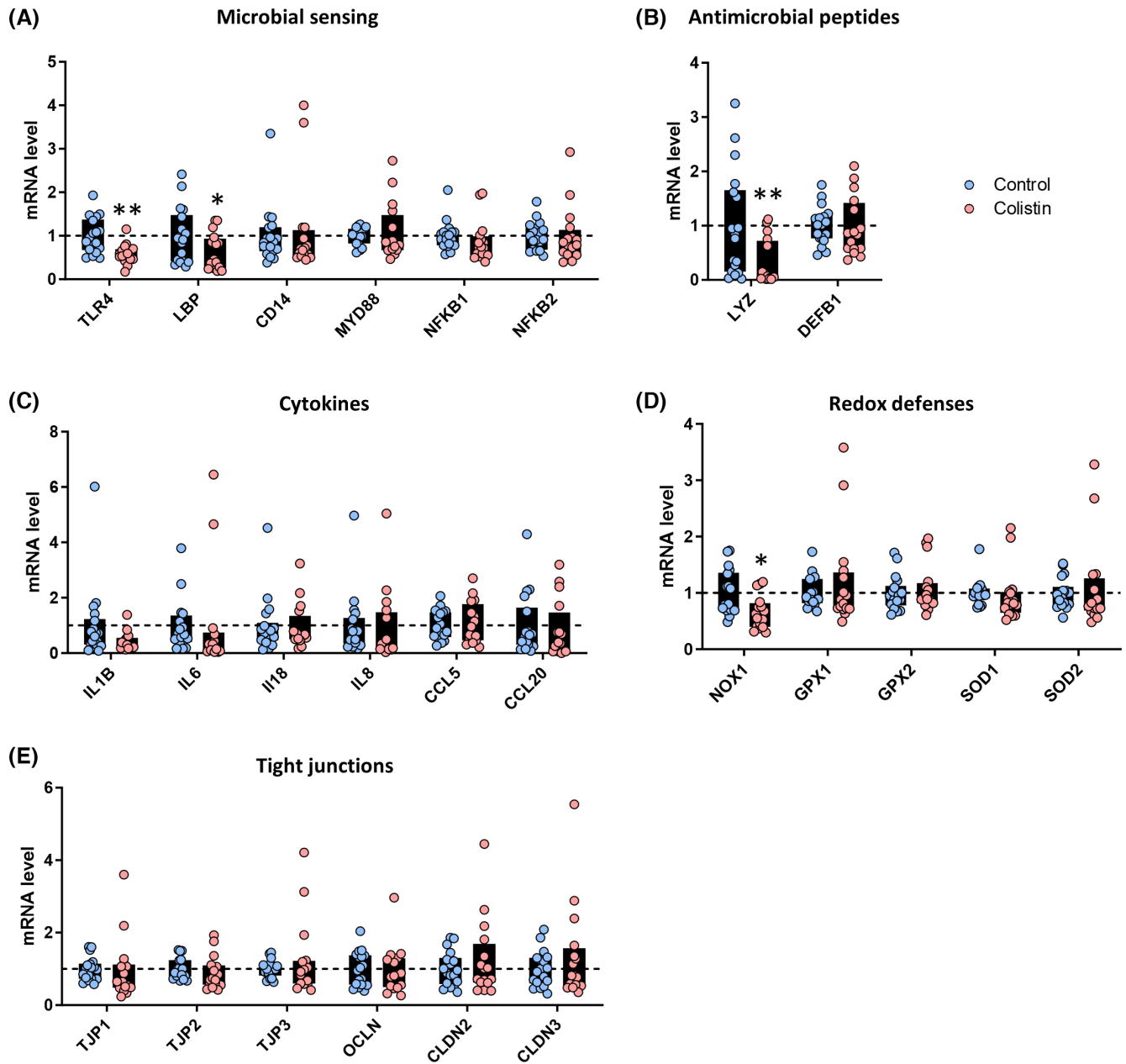
FIGURE 4 Innate immune defenses are reduced in the colon epithelium of neonatal piglets treated with colistin. Piglets were treated from birth to day 7 orally with colistin ($n = 16$) or water (control group, $n = 18$). (A–E) Gene expression was analyzed by qPCR in colon epithelial cells. Relative expression of genes coding for proteins involved in microbial sensing (A), antimicrobial peptides (B), cytokines (C), proteins involved in redox homeostasis (D), and tight junctions (E). (A–E) Each dot represents an individual value. Boxes extend from the 25th to the 75th percentiles. Significant differences are represented as **$p < .01$, *$p < .05$ (colistin vs. control).

overall disruption of the colon microbiota. However, some of these effects might be attributed to (i) an increased exposure to microbiota-derived succinate, or (ii) a reduced exposure to LPS, or (iii) a direct action of colistin on intestinal epithelial cells. To test these three hypotheses, we treated colon organoid cell monolayers derived from epithelial crypts collected immediately after birth (i.e., before significant microbial colonization of the pig colon) with succinate (0.1, 1,

and 10 mM), LPS (0.1, 1, and 10 μg/mL), and colistin (1, 10, and 100 μg/mL) (Figure 5A).

Organoid cell monolayers were fully confluent and characterized by a high TEER value (>2000 Ohm.cm²). The treatments did not alter the morphology of the cell monolayers nor the TEER (Figure 5B,C), indicating no modification of the epithelial barrier function. We then evaluated whether succinate, LPS, or colistin altered the expression of some genes that were regulated in vivo upon
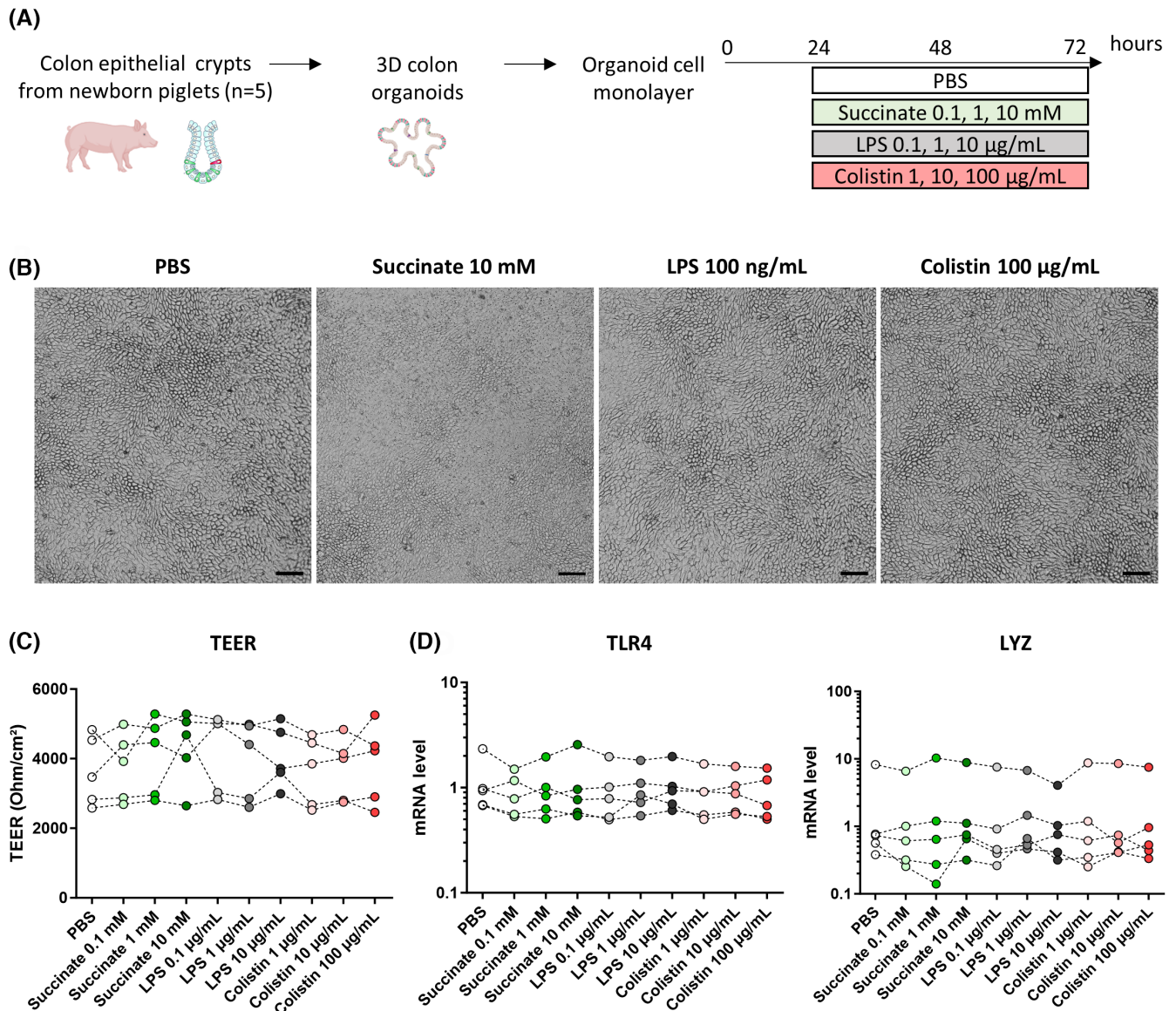
FIGURE 5 Succinate, lipopolysaccharide, and colistin do not alter epithelial barrier function in organoid cell monolayers derived from the colon of newborn piglets. Organoid cell monolayers derived from the colon of newborn piglets ($n = 5$) were treated for 48 h with PBS (negative control) or succinate (0.1, 1, and 10 mM), lipopolysaccharide (LPS—1, 10, and 100 ng/µL) or colistin (1, 10, and 100 µg/mL). The transepithelial electrical resistance (TEER) was measured and gene expression was analyzed by qPCR in cell monolayers 48 h after treatment. (A) Schematic representation of the experimental design. (B) Representative brightfield microscopic images of organoid cell monolayers 48 h after treatment with PBS or with the highest concentration tested of succinate, LPS, and colistin (scale bar: 100 µm). (C) TEER. (D) Relative gene expression of TLR4 and LYZ. (C, D) Each dot represents a value measured in one organoid cell monolayer. Organoid cell monolayers derived from the same piglet are linked by a dotted line. No significant differences were found for the parameters presented in this figure.

disruption of the primocolonizing microbiota. We found that the expression levels of TLR4 and LYZ were similar in all conditions (Figure 5D). Treatments had also no effect on the gene expression of PYY and PCNA (data not shown). Thus, our results suggest that the modification of colon epithelial functions observed in vivo after disruption of the primocolonizing microbiota is not directly driven by the exposure to variable levels of succinate or LPS nor to colistin and rather results from the overall modification of the microbial environment.

3.5 | Disruption of the primocolonizing microbiota imprints epithelial stem cells in the colon

We hypothesized that the modification of the primocolonizing microbiota might have long-term consequences for intestinal homeostasis through imprinting of epithelial stem cells. Thus, we cultivated colon organoids derived from cryopreserved crypt stem cells collected from a subset of control and colistin-treated piglets, selected based

on their high and low in vivo expression of TLR4 and LYZ, respectively ($n = 9$/group) (Figure 6A). Organoids were passaged twice in sterile conditions in order to ensure the lack of residual microbial stimuli. Colon organoids from both control and colistin-treated piglets displayed a typical morphology with budding or spherical morphologies (Figure 6B). No differences in growth or morphology were observed between organoids derived from control or colistin-treated piglets.

We analyzed, in colon organoids after two passages, the expression of genes whose expressions were modified in epithelial crypts in vivo by the colistin-induced modification of the primocolonizing microbiota. The in vitro gene expression of LYZ and TLR4 was lower in colon organoids derived from piglets treated with colistin when compared to control piglets as observed in vivo (Figure 6C). In contrast, the other genes modulated in vivo were found

expressed at a similar level in organoids derived from control or colistin-treated piglets. Thus, our results show that the modification of the primocolonizing microbiota induced by colistin in vivo imprinted to some extent stem cells in the colon epithelium of neonatal piglets.

Finally, in order to explore the mechanisms underlying the imprinting of epithelial stem cells, we selected three piglets from the control group with a high expression of LYZ and three piglets from the colistin group with a low expression of LYZ. The gene expression of LYZ was analyzed in the colon organoids derived from these piglets at two additional passages (Figure 7A). The LYZ expression profile observed in vivo was maintained in organoids at each passage (Figure 7B). We hypothesized that the imprinting of LYZ gene expression involved the trimethylation of histone H3 lysine 4 (H3K4me3), an epigenetic mark associated with gene activation. Indeed, a previous study
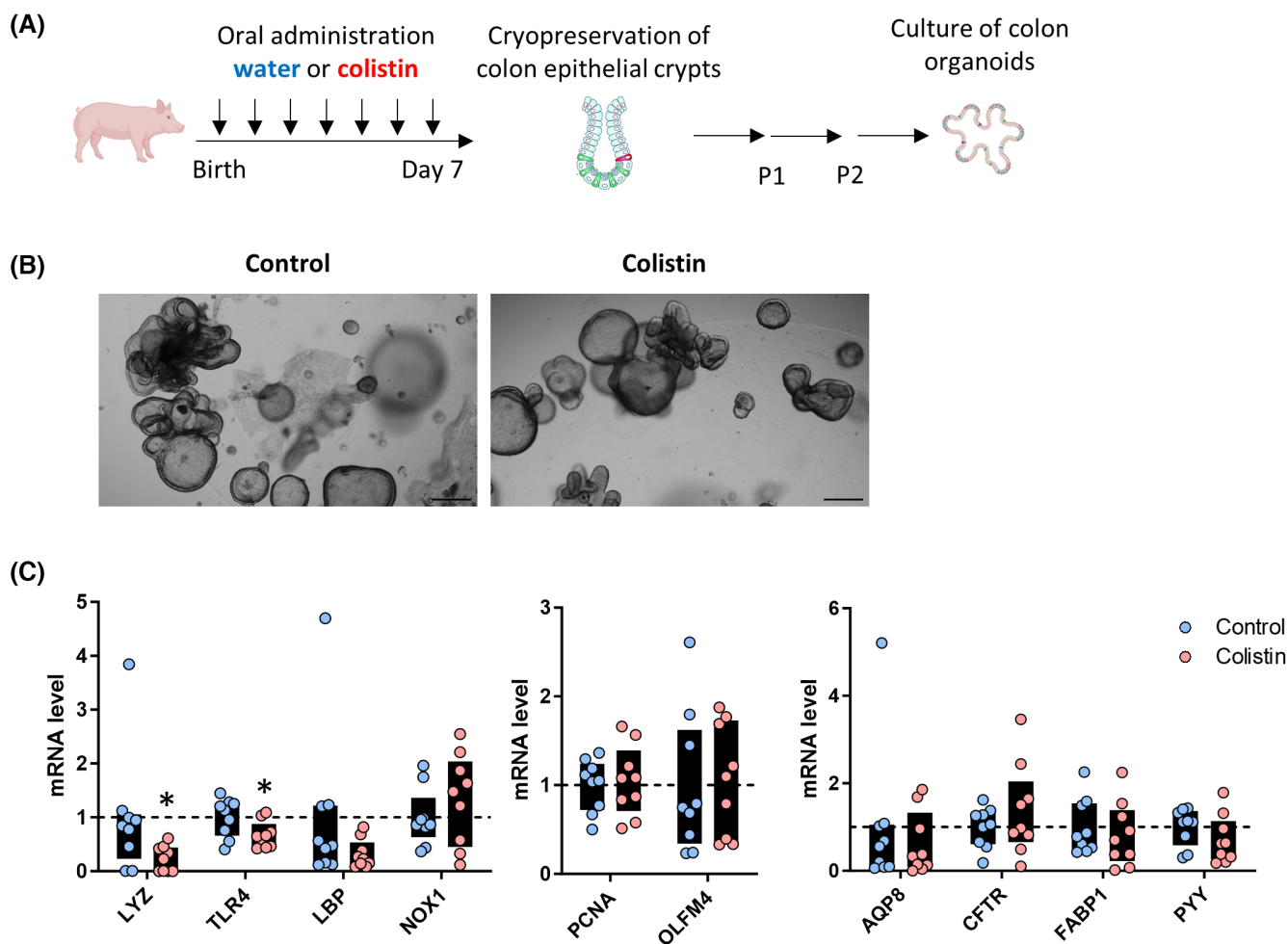

FIGURE 6 Colon epithelial stem cells are imprinted in neonatal piglets treated with colistin. Colon organoids were obtained from cryopreserved epithelial crypts isolated from a subset of piglets treated for 7 days with colistin ($n = 9$) or water ($n = 9$). After two passages, gene expression was analyzed in organoids by qPCR. (A) Schematic representation of the experimental design. (B) Representative brightfield microscopic images of organoids (scale bar: 500 μm). (C) Relative expression levels of genes involved in innate immunity, epithelial renewal, and differentiation. Each dot represents an individual value. Boxes extend from the 25th to the 75th percentiles. Significant differences are represented as *$p < .05$ (colistin vs. control).
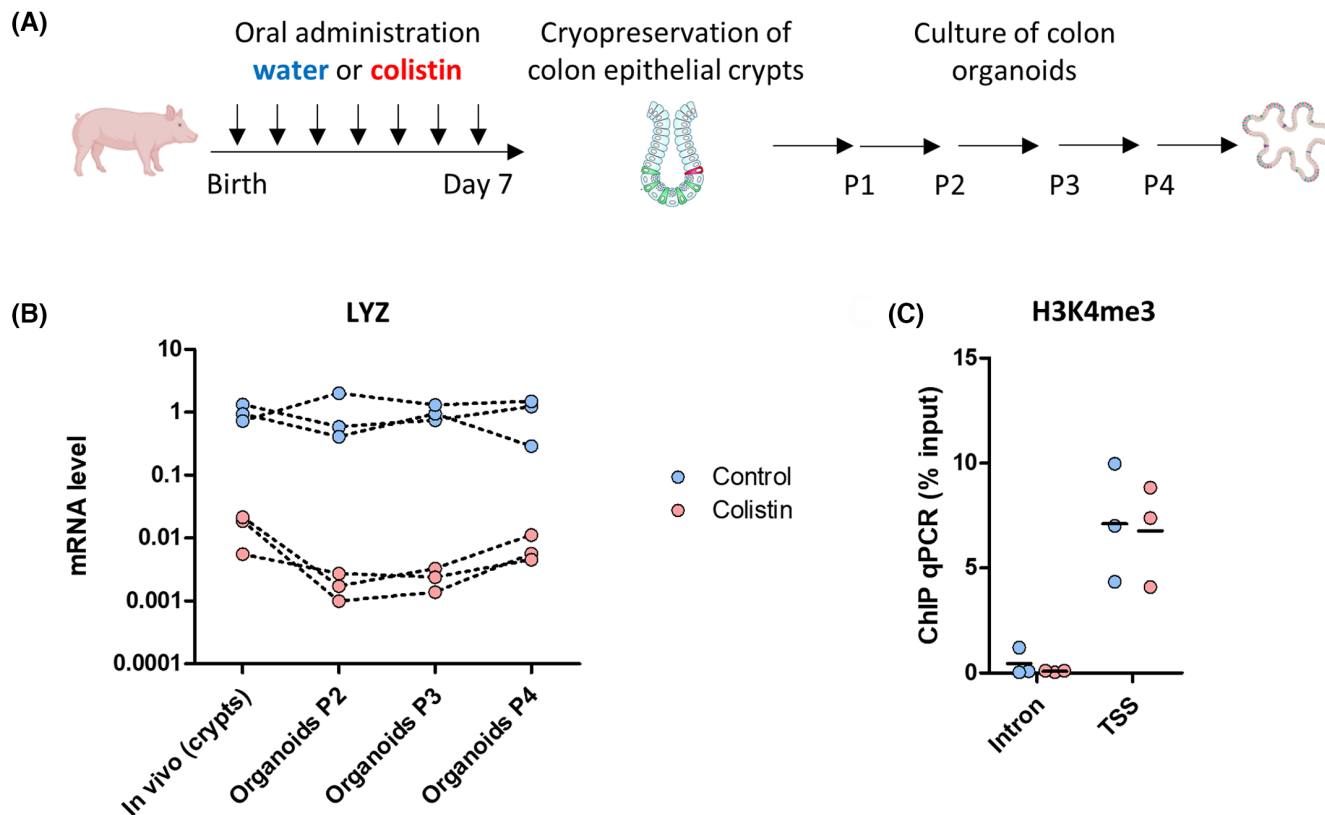
FIGURE 7 The stable imprinting of lysozyme in colon organoids is independent of H3K4me3. Colon organoids derived from a subset of piglets treated for 7 days with colistin ($n = 3$) or water ($n = 3$) were selected based on their low and high expression of lysozyme (LYZ), respectively. Organoids cryopreserved after two passages (P2) were thawed and cultured for two additional passages (P3 and P4). (A) Schematic representation of the experimental design. (B) LYZ gene expression was analyzed by qPCR in colon epithelial crypts and in organoids at passages P2, P3, and P4. Each dot represents an individual value. Samples derived from the same piglet are linked by a dotted line. (C) Histone 3 lysine 4 trimethylation (H3K4me3) level was quantified in the LYZ transcription start site (TSS) and in an intronic region (negative control) by chromatin immunoprecipitation (ChIP)-qPCR. The results were normalized to the level of target DNA measured in the input sample (non-immunoprecipitated). Dots and bars represent individual and mean values, respectively.

linked abundant H3K4me3 at the promoter of LYZ gene in cell types expressing high level of this gene.[45] ChIP-qPCR was performed in the organoid lines for which LYZ mRNA levels were assessed. As expected, H3K4me3 abundance was higher in the LYZ transcription start site (TSS) when compared to an intronic region (Figure 7C). However, the abundance of H3K4me3 in LYZ TSS was similar between the organoids with high and low LYZ gene expression derived from control and colistin-treated piglets, respectively. Thus, the imprinting of LYZ in organoid cells involves other epigenetic modifications than H3K4me3.

4 | DISCUSSION

The aim of our study was to evaluate the consequences for the intestinal epithelium of the depletion of specific gram-negative bacteria that are transiently dominant in the neonatal gut microbiota. For that, we used colistin (Polymyxin E), which is an antibiotic poorly absorbed in the gut and that

exerts antimicrobial activity through its binding to the LPS of gram-negative bacteria and which is commonly used in pigs to treat infection by *Enterobacteriaceae*.[42] The specific depletion of Proteobacteria (mostly *Enterobacteriaceae* and *Pasteurellaceae*) and Fusobacteriota (*Fusobacteriacae*) induced by colistin in the colon microbiota of neonatal piglets is consistent with the mode of action of this antibiotic and with other studies in pigs.[26] Importantly, colistin did not reduce the overall microbiota richness and diversity and did not promote a compensatory bloom of specific bacteria, which is in agreement with previous studies in mice and pigs.[46,47] Thus, our model of neonatal piglets treated with colistin during the first week of life is suitable to investigate the consequences for the colon epithelium of the lack of postnatal colonization of the gut by Proteobacteria and Fusobacteriota, which are typically transiently dominant (>20%) in the colon of neonatal piglets.[48]

The depletion of *Enterobacteriaceae* induced by colistin was associated with a reduction of the predicted capacity of the primocolonizing microbiota to

biosynthesize LPS and enterobactin, which can both trigger epithelial innate immune responses upon sensing by intestinal epithelial cells.[49] Accordingly, the epithelial expression of the LPS sensors TLR4 and LBP and the downstream antimicrobial proteins LYZ and NOX1 were reduced in piglets treated with colistin.[50] In agreement with our results, a study showed that microinjection of human intestinal organoids with non-pathogenic *E. coli* up-regulated TLR signaling and antimicrobial peptide production.[51] The reduced expression of the stem cell and proliferation markers (OLFM4, PNCA) in the colon of piglets treated with colistin could be linked to the reduced TLR4 signaling that was previously shown to promote epithelial proliferation.[51,52] The similar crypt depth between piglets treated or not with colistin suggests that the lower proliferation rate might be compensated by increased apoptosis or that the effect at the gene expression level did not translate yet into morphological modifications during the short period of treatment (7 days). Interestingly, mono-colonization of germ-free rats and pigs by non-pathogenic *E. coli* also stimulated proliferation of intestinal epithelial cells.[22,53] The Notch pathway that determines epithelial cell fate is also controlled by TLR signaling,[50] which could explain the regulation of genes involved in absorptive and secretory functions in the colon epithelium of neonatal piglets treated with colistin. We hypothesized that the reduced sensing of compounds derived from gram-negative bacteria (e.g., LPS) could drive the modifications of epithelial gene expression observed in the colon of piglets treated with colistin. However, LPS had no effect on TEER and gene expression in colon organoid cell monolayers derived from vaginally born neonatal piglets, which could be explained by the development immediately after birth of tolerance to LPS by intestinal epithelial cells.[54] Accordingly, cell monolayers derived from fetal human organoid were responsive to LPS while cells derived from the adult intestine were not.[36]

The accumulation of succinate in the colon upon disruption of the primocolonizing gut microbiota by colistin is in line with previous studies reporting high concentration of succinate in pigs and in mice treated with antibiotics.[55,56] Succinate is a metabolic intermediate in bacterial synthesis of propionate.[57] Accordingly, we also observed that colistin reduced the propionate concentration in the colon of piglets. This metabolic shift could be explained by the depletion of *E. coli* whose genome encodes enzymes that decarboxylate succinate to propionate.[58] We hypothesized that succinate accumulation could be involved in the modulation of epithelial functions since this bacterial metabolite was previously shown to reduce intestinal inflammation and epithelial permeability.[33,59] However, we found no effect of succinate (0.1–10 mM) on organoid cell

monolayers derived from newborn piglets. These results might be explained by the scarcity of tuft cells in conventional culture condition of intestinal organoids.[60] Indeed, previous studies showed that tuft cells mediate the effects of succinate on the gut barrier.[59,61,62] We also tested whether the alteration of gene expression in the colon epithelium could have been driven by a direct effect of colistin since previous studies showed that other antibiotics altered the expression of antimicrobial peptides and impaired mitochondrial metabolism in epithelial cells.[7,63] However, our results obtained in organoid cell monolayers suggest that a direct action of colistin on colon epithelial cells is unlikely. Although we did not identify a precise molecular mechanism, the reduction of innate immune responses in the colon epithelium of colistin-treated piglets probably involves a reduced exposure to compounds derived from gram-negative Proteobacteria and Fusobacteriota.

Our experiments in colon organoids revealed that the disruption of the primocolonizing microbiota induced by colistin-imprinted intestinal epithelial stem cells. Indeed, the expression of LYZ and TLR4 remained reduced in organoids derived from piglets treated with colistin, even after several passages that ensured the elimination of residual microbiota-derived compounds. These results are in line with previous studies showing that tissue-derived intestinal organoids retained some transcriptomic signatures specific to the gut region[38,64–66] and to the disease state.[67,68] In contrast, other studies showed that organoids derived from germ-free or conventional mice did not retain the transcriptomic differences observed in vivo.[69,70] This variable capacity of intestinal organoids to retain gene expression patterns observed in the tissue of origin might be related to gene-specific regulations. Indeed, we observed that organoids derived from colistin-treated piglets did not retain the expression pattern of genes other than LYZ and TLR4, which suggests that the in vivo expression pattern of these genes that are not retained in organoids could require microbial signals (e.g., NOX1, LBP) or be erased under the influence of the proliferation-promoting culture medium (e.g., OLFM4, PCNA).

The ability of intestinal organoids to retain some transcriptomic features of their tissue of origin involves epigenetic imprinting.[71] Since the gut microbiota was previously shown to alter H3K4me3 in genes involved in antimicrobial responses in mouse intestinal epithelial cells[72] and considering that this epigenetic mark of transcriptionally active chromatin was previously shown to regulate LYZ expression,[45] we hypothesized that this mechanism could be involved in the imprinting of LYZ in colon stem cells upon disruption of the primocolonizing microbiota. However, we found that the stable imprinting of LYZ in organoids was not linked to the level of H3K4me3 in its promoter region. Other epigenetic modifications such as DNA methylation

might, thus, underlie the imprinting of epithelial stem cells induced by colistin, as demonstrated for the maintenance of regional identity in human organoids.[65]

In conclusion, our results show that a disruption of the neonatal gut microbiota characterized by the depletion of Proteobacteria and Fusobacteriota altered epithelial functions notably by reducing epithelial innate immune defenses. We also demonstrated that disruption of the neonatal gut microbiota imprinted colon epithelial stem cells, which could have long-term consequences for intestinal homeostasis since stem cells are long-lived and are responsible for the constant renewal of the epithelium. Thus, further experiments will be required to determine the long-term consequences for the gut barrier of the lack of neonatal colonization by Proteobacteria and Fusobacteriota, notably upon inflammatory or infectious challenges.

AUTHOR CONTRIBUTIONS

ACKNOWLEDGMENTS

DISCLOSURES

The authors declare no conflict of interest for the work presented in this article.

DATA AVAILABILITY STATEMENT

Sequencing reads were deposited in the National Center for Biotechnology Information Sequence Read Archive (accession number: PRJNA933391).

ORCID

Martin Beaumont https://orcid.org/0000-0002-1559-2067
Katia Fève https://orcid.org/0000-0003-3287-1604
Sylvie Combes https://orcid.org/0000-0002-2945-4423
Guillaume Devailly https://orcid.org/0000-0001-8878-9357
Gaëlle Boudry https://orcid.org/0000-0002-5287-571X

REFERENCES

1. Peterson LW, Artis D. Intestinal epithelial cells: regulators of barrier function and immune homeostasis. *Nat Rev Immunol*. 2014;14:141-153.
2. Elmentaite R, Kumasaka N, Roberts K, et al. Cells of the human intestinal tract mapped across space and time. *Nature*. 2021;597:250-255.
3. Gehart H, Clevers H. Tales from the crypt: new insights into intestinal stem cells. *Nat Rev Gastroenterol Hepatol*. 2019;16:19-34.
4. Frazer LC, Good M. Intestinal epithelium in early life. *Mucosal Immunol*. 2022;15:1181-1187.
5. Schumann A, Nutten S, Donnicola D, et al. Neonatal antibiotic treatment alters gastrointestinal tract developmental gene expression and intestinal barrier transcriptome. *Physiol Genomics*. 2005;23:235-245. doi:10.1152/physiolgenomics.00057.2005
6. Hughes KR, Schofield Z, Dalby MJ, et al. The early life microbiota protects neonatal mice from pathological small intestinal epithelial cell shedding. *FASEB J*. 2020;34:7075-7088.
7. Garcia TM, van Roest M, Vermeulen JLM, et al. Early life antibiotics influence in vivo and in vitro mouse intestinal epithelium maturation and functioning. *Cell Mol Gastroenterol Hepatol*. 2021;12:943-981.
8. Chaaban H, Patel MM, Burge K, et al. Early antibiotic exposure alters intestinal development and increases susceptibility to necrotizing enterocolitis: a mechanistic study. *Microorganisms*. 2022;10:519.
9. Pan W-H, Sommer F, Falk-Paulsen M, et al. Exposure to the gut microbiota drives distinct methylome and transcriptome changes in intestinal epithelial cells during postnatal development. *Genome Med*. 2018;10:27.
10. Heppert JK, Davison JM, Kelly C, Mercado GP, Lickwar CR, Rawls JF. Transcriptional programmes underlying cellular identity and microbial responsiveness in the intestinal epithelium. *Nat Rev Gastroenterol Hepatol*. 2021;18:7-23.
11. Dougherty MW, Kudin O, Mühlbauer M, Neu J, Gharaibeh RZ, Jobin C. Gut microbiota maturation during early human life induces enterocyte proliferation via microbial metabolites. *BMC Microbiol*. 2020;20:205.
12. Beaumont M, Paës C, Mussard E, et al. Gut microbiota derived metabolites contribute to intestinal barrier maturation at the suckling-to-weaning transition. *Gut Microbes*. 2020;11:1268-1286.
13. Roager HM, Stanton C, Hall LJ. Microbial metabolites as modulators of the infant gut microbiome and host-microbial interactions in early life. *Gut Microbes*. 2023;15:2192151.
14. Lee Y-S, Kim T-Y, Kim Y, et al. Microbiota-derived lactate accelerates intestinal stem-cell-mediated epithelial development. *Cell Host Microbe*. 2018;24:833-846.e6.
15. Krautkramer KA, Dhillon RS, Denu JM, Carey HV. Metabolic programming of the epigenome: host and gut microbial metabolite interactions with host chromatin. *Transl Res*. 2017;189:30-50.

16. Woo V, Alenghat T. Epigenetic regulation by gut microbiota. *Gut Microbes*. 2022;14:2022407.

17. Shin N-R, Whon TW, Bae J-W. Proteobacteria: microbial signature of dysbiosis in gut microbiota. *Trends Biotechnol*. 2015;33:496-503.

18. Bäckhed F, Roswall J, Peng Y, et al. Dynamics and stabilization of the human gut microbiome during the first year of life. *Cell Host Microbe*. 2015;17:690-703.

19. Laforest-Lapointe I, Arrieta M-C. Patterns of early-life gut microbial colonization during human immune development: an ecological perspective. *Front Immunol*. 2017;8:788. doi:10.3389/fimmu.2017.00788

20. Derrien M, Alvarez A-S, de Vos WM. The gut microbiota in the first decade of life. *Trends Microbiol*. 2019;27:997-1010.

21. Tsukuda N, Yahagi K, Hara T, et al. Key bacterial taxa and metabolic pathways affecting gut short-chain fatty acid profiles in early life. *ISME J*. 2021;15:2574-2590.

22. Tomas J, Reygner J, Mayeur C, et al. Early colonizing *Escherichia coli* elicits remodeling of rat colonic epithelium shifting toward a new homeostatic state. *ISME J*. 2015;9:46-58.

23. Heinritz SN, Mosenthin R, Weiss E. Use of pigs as a potential model for research into dietary modulation of the human gut microbiota. *Nutr Res Rev*. 2013;26:191-209.

24. Roura E, Koopmans S-J, Lallès J-P, et al. Critical review evaluating the pig as a model for human nutritional physiology. *Nutr Res Rev*. 2016;29:60-90.

25. Walthall K, Cappon GD, Hurtt ME, Zoetis T. Postnatal development of the gastrointestinal system: a species comparison. *Birth Defects Res B Dev Reprod Toxicol*. 2005;74:132-156.

26. Fleury MA, Jouy E, Eono F, et al. Impact of two different colistin dosing strategies on healthy piglet fecal microbiota. *Res Vet Sci*. 2016;107:152-160.

27. Read T, Fortun-Lamothe L, Pascal G, et al. Diversity and co-occurrence pattern analysis of cecal microbiota establishment at the onset of solid feeding in young rabbits. *Front Microbiol*. 2019;10:973.

28. Escudié F, Auer L, Bernard M, et al. FROGS: find, rapidly, OTUs with galaxy solution. *Bioinformatics*. 2018;34:1287-1294.

29. Douglas GM, Maffei VJ, Zaneveld JR, et al. PICRUSt2 for prediction of metagenome functions. *Nat Biotechnol*. 2020;38:685-688.

30. Darbot V, Samb M, Bernard M, Rué O, Pascal G. FROGSFUNC: smart integration of PICRUSt2 software into FROGS pipeline. *JOBIM*. 2022; [Internet] 2022. Accessed February 8, 2023. https://hal.inrae.fr/hal-03806133

31. Guitton Y, Tremblay-Franco M, Le Corguillé G, et al. Create, run, share, publish, and reference your LC–MS, FIA–MS, GC–MS, and NMR data analysis workflows with the Workflow4Metabolomics 3.0 galaxy online infrastructure for metabolomics. *Int J Biochem Cell Biol*. 2017;93:89-101.

32. Mussard E, Lencina C, Boudry G, et al. Culture of piglet intestinal 3D organoids from cryopreserved epithelial crypts and establishment of cell monolayers. *J Vis Exp*. 2023;(192):e64917. doi:10.3791/64917

33. Li X, Mao M, Zhang Y, Yu K, Zhu W. Succinate modulates intestinal barrier function and inflammation response in pigs. *Biomolecules*. 2019;9:486.

34. Fremder M, Kim SW, Khamaysi A, et al. A transepithelial pathway delivers succinate to macrophages, thus perpetuating their pro-inflammatory metabolic state. *Cell Rep*. 2021;36:109521.

35. Bauset C, Lis-Lopez L, Coll S, et al. SUCNR1 mediates the priming step of the inflammasome in intestinal epithelial cells: relevance in ulcerative colitis. *Biomedicine*. 2022;10:532.

36. Senger S, Ingano L, Freire R, et al. Human fetal-derived enterospheres provide insights on intestinal development and a novel model to study necrotizing enterocolitis (NEC). *Cell Mol Gastroenterol Hepatol*. 2018;5:549-568.

37. Ruan W, Engevik MA, Chang-Graham AL, et al. Enhancing responsiveness of human jejunal enteroids to host and microbial stimuli. *J Physiol*. 2020;598:3085-3105.

38. Kayisoglu O, Weiss F, Niklas C, et al. Location-specific cell identity rather than exposure to GI microbiota defines many innate immune signalling cascades in the gut epithelium. *Gut*. 2021;70:687-697.

39. Guyonnet J, Manco B, Baduel L, Kaltsatos V, Aliabadi MHFS, Lees P. Determination of a dosage regimen of colistin by pharmacokinetic/pharmacodynamic integration and modeling for treatment of G.I.T. disease in pigs. *Res Vet Sci*. 2010;88:307-314.

40. Peng C, Zuo S, Qiu Y, Fu S, Peng L. Determination of colistin in contents derived from gastrointestinal tract of feeding treated piglet and broiler. *Antibiotics*. 2021;10:422.

41. Paës C, Gidenne T, Bébin K, et al. Early introduction of solid feeds: ingestion level matters more than prebiotic supplementation for shaping gut microbiota. *Front Vet Sci*. 2020;7:261. doi:10.3389/fvets.2020.00261

42. Rhouma M, Beaudry F, Thériault W, Letellier A. Colistin in pig production: chemistry, mechanism of antibacterial action, microbial resistance emergence, and one health perspectives. *Front Microbiol*. 2016;7:1789. doi:10.3389/fmicb.2016.01789

43. Bian G, Ma S, Zhu Z, et al. Age, introduction of solid feed and weaning are more important determinants of gut bacterial succession in piglets than breed and nursing mother as revealed by a reciprocal cross-fostering model. *Environ Microbiol*. 2016;18:1566-1577.

44. Liu H, Zeng X, Zhang G, et al. Maternal milk and fecal microbes guide the spatiotemporal development of mucosa-associated microbiota and barrier function in the porcine neonatal gut. *BMC Biol*. 2019;17:106.

45. Polo JM, Liu S, Figueroa ME, et al. Cell type of origin influences the molecular and functional properties of mouse induced pluripotent stem cells. *Nat Biotechnol*. 2010;28:848-855.

46. Sovran B, Planchais J, Jegou S, et al. Enterobacteriaceae are essential for the modulation of colitis severity by fungi. *Microbiome*. 2018;6:152.

47. Rhouma M, Braley C, Thériault W, Thibodeau A, Quessy S, Fravalo P. Evolution of pig fecal microbiota composition and diversity in response to enterotoxigenic *Escherichia coli* infection and colistin treatment in weaned piglets. *Microorganisms*. 2021;9:1459.

48. Arnaud AP, Rome V, Richard M, Formal M, David-Le Gall S, Boudry G. Post-natal co-development of the microbiota and gut barrier function follows different paths in the small and large intestine in piglets. *FASEB J*. 2020;34:1430-1446.

49. Saha P, Yeoh BS, Xiao X, et al. Enterobactin induces the chemokine, interleukin-8, from intestinal epithelia by chelating intracellular iron. *Gut Microbes*. 2020;12:1841548.

50. Burgueño JF, Abreu MT. Epithelial toll-like receptors and their role in gut homeostasis and disease. *Nat Rev Gastroenterol Hepatol*. 2020;17:263-278.

51. Hill DR, Huang S, Nagy MS, et al. Bacterial colonization stimulates a complex physiological response in the immature human intestinal epithelium. *Elife*. 2017;6:e29132.

52. Sodhi CP, Neal MD, Siggers R, et al. Intestinal epithelial toll-like receptor 4 regulates goblet cell development and is required for necrotizing enterocolitis in mice. *Gastroenterology*. 2012;143:708-718.e5.

53. Danielsen M, Hornshøj H, Siggers RH, Jensen BB, van Kessel AG, Bendixen E. Effects of bacterial colonization on the porcine intestinal proteome. *J Proteome Res*. 2007;6:2596-2604.

54. Lotz M, Gütle D, Walther S, Ménard S, Bogdan C, Hornef MW. Postnatal acquisition of endotoxin tolerance in intestinal epithelial cells. *J Exp Med*. 2006;203:973-984.

55. Tsukahara T, Ushida K. Succinate accumulation in pig large intestine during antibiotic-associated diarrhea and the constitution of succinate-producing flora. *J Gen Appl Microbiol*. 2002;48:143-154.

56. Ferreyra JA, Wu KJ, Hryckowian AJ, Bouley DM, Weimer BC, Sonnenburg JL. Gut microbiota-produced succinate promotes *C. difficile* infection after antibiotic treatment or motility disturbance. *Cell Host Microbe*. 2014;16:770-777.

57. Louis P, Flint HJ. Formation of propionate and butyrate by the human colonic microbiota. *Environ Microbiol*. 2017;19:29-41.

58. Haller T, Buckel T, Rétey J, Gerlt JA. Discovering new enzymes and metabolic pathways: conversion of succinate to propionate by *Escherichia coli*. *Biochemistry*. 2000;39:4622-4629.

59. Banerjee A, Herring CA, Chen B, et al. Succinate produced by intestinal microbes promotes specification of tuft cells to suppress ileal inflammation. *Gastroenterology*. 2020;159:2101-2115.e5.

60. Boonekamp KE, Dayton TL, Clevers H. Intestinal organoids as tools for enriching and studying specific and rare cell types: advances and future directions. *J Mol Cell Biol*. 2020;12:562-568.

61. Lei W, Ren W, Ohmoto M, et al. Activation of intestinal tuft cell-expressed Sucnr1 triggers type 2 immunity in the mouse small intestine. *Proc Natl Acad Sci*. 2018;115:5552-5557.

62. Nadjsombati MS, McGinty JW, Lyons-Cohen MR, et al. Detection of succinate by intestinal tuft cells triggers a type 2 innate immune circuit. *Immunity*. 2018;49:33-41.e7.

63. Morgun A, Dzutsev A, Dong X, et al. Uncovering effects of antibiotics on the host and microbiota using transkingdom gene networks. *Gut*. 2015;64:1732-1743.

64. Middendorp S, Schneeberger K, Wiegerinck CL, et al. Adult stem cells in the small intestine are intrinsically programmed with their location-specific function. *Stem Cells*. 2014;32:1083-1091.

65. Kraiczy J, Nayak KM, Howell KJ, et al. DNA methylation defines regional identity of human intestinal epithelial organoids and undergoes dynamic changes during development. *Gut*. 2019;68:49-61.

66. Mussard E, Lencina C, Gallo L, et al. The phenotype of the gut region is more stably retained than developmental stage in piglet intestinal organoids. *Front Cell Dev Biol*. 2022;10:983031. doi:10.3389/fcell.2022.983031

67. Dotti I, Mora-Buch R, Ferrer-Picón E, et al. Alterations in the epithelial stem cell compartment could contribute to permanent changes in the mucosa of patients with ulcerative colitis. *Gut*. 2017;66:2069-2079.

68. Howell KJ, Kraiczy J, Nayak KM, et al. DNA methylation and transcription patterns in intestinal epithelial cells from pediatric patients with inflammatory bowel diseases differentiate disease subtypes and associate with outcome. *Gastroenterology*. 2018;154:585-598.

69. Janeckova L, Kostovcikova K, Svec J, et al. Unique gene expression signatures in the intestinal mucosa and organoids derived from germ-free and monoassociated mice. *Int J Mol Sci*. 2019;20:E1581.

70. Hausmann A, Russo G, Grossmann J, et al. Germ-free and microbiota-associated mice yield small intestinal epithelial organoids with equivalent and robust transcriptome/proteome expression phenotypes. *Cell Microbiol*. 2020;22:e13191.

71. Kraiczy J, Zilbauer M. Intestinal epithelial organoids as tools to study epigenetics in gut health and disease. *Stem Cells Int*. 2019;2019:7242415.

72. Kelly D, Kotliar M, Woo V, et al. Microbiota-sensitive epigenetic signature predicts inflammation in Crohn's disease. *JCI Insight*. 2018;3(18):e122104.

SUPPORTING INFORMATION

Additional supporting information can be found online in the Supporting Information section at the end of this article.

How to cite this article: Beaumont M, Lencina C, Fève K, et al. Disruption of the primocolonizing microbiota alters epithelial homeostasis and imprints stem cells in the colon of neonatal piglets. *The FASEB Journal*. 2023;37:e23149. doi:10.1096/fj.202301182R